Journal of Multiscale Modelling
Vol. 6, No. 1 (2015) 1450001 (22 pages)

DOI: 10.1142/S1756973714500012

Imperial College Press
www.icpress.co.uk

A Dynamic Adaptive Wavelet Method for Solution of the Schrodinger Equation

Ratikanta Behera* and Mani Mehra†

Department of Mathematics
Indian Institute of Technology
New Delhi-110016, India
**rbehera@nd.edu*
†*mmehra@maths.iitd.ac.in*

Published 15 June 2015

In this paper, we present a dynamically adaptive wavelet method for solving Schrodinger equation on one-dimensional, two-dimensional and on the sphere. Solving one-dimensional and two-dimensional Schrodinger equations are based on Daubechies wavelet with finite difference method on an arbitrary grid, and for spherical Schrodinger equation is based on spherical wavelet over an optimal spherical geodesic grid. The method is applied to the solution of Schrodinger equation for computational efficiency and achieve accuracy with controlling spatial grid adaptation — high resolution computations are performed only in regions where a solution varies greatly (i.e., near steep gradients, or near-singularities) and a much coarser grid where the solution varies slowly. Thereupon the dynamic adaptive wavelet method is useful to analyze local structure of solution with very less number of computational cost than any other methods. The prowess and computational efficiency of the adaptive wavelet method is demonstrated for the solution of Schrodinger equation on one-dimensional, two-dimensional and on the sphere.

Keywords: Schrodinger equation; adaptive wavelet method; spherical wavelet; Daubechies wavelet.

1. Introduction

The rapid expansion in computational power has fueled a broad range investigation into the efficiency of various algorithms for the solution of general classes of partial differential equations (PDEs). Many of these PDEs exhibit localized high frequency behavior. The conventional finite difference approach is most widely used technique to solve PDEs numerically, however it requires a very fine grid to incorporate the steep gradients. The disadvantage of the finite difference approach has required very large number of grid points which heavily increases the computational cost. Furthermore, most of these grid points are located in regions where the solution is quite smooth and such a fine grid is not required there. To avoid this problem, proper adaptive grid is needed. In the proposed wavelet method in Refs. 19, 18 and 24, the wavelet coefficients are used to place nonuniform grids adaptively.

The nonlinear Schrodinger equation arises in several areas of physics, such as quantum mechanics (modeling of quantum devices[2,3]), electromagnetic wave propagation,[21] quantum treatment of the nuclei,[32] underwater acoustics (paraxial approximations to the wave equation[30]). In mathematics, the Schrodinger equation and its variants is one of the basic equations studied in the field of PDEs,[1,16] and has applications to geometry, to spectral and scattering theory, and to integrable systems.[1] Since the nonlinear Schrodinger equation is a parabolic equation, it resembles in the form of standard diffusion equation. There is a significant physical difference, of course, since the solution diffuses in imaginary time and is not naturally thus dispersion becomes a critical numerical issue. There have been several numerical methods to obtained the solution of nonlinear Schrodinger equation on one-dimensional, two-dimensional and sphere (i.e., discontinuous Galerkin method,[17] finite-difference representation,[7] symplectic and multi-symplectic wavelet collocation method,[39] interpolating wavelet method,[27] multiwavelet bases optimization of finite difference method,[31] spectral-element method,[20] spectral grid method,[22] and spectral basis and effects of split-operator technique,[29] Fourier transform methods[11]). Of course variety of methods are available that can compute accurate numerical approximations of the physically relevant solutions. But in recent years, wavelet methods have becomes a powerful tool for the problems arising different areas of science and engineering. Wavelet methods have been developed for other application in Refs. 6 and 37.

As finite-difference, finite-volume and finite-element methods have small compact support but poor continuity properties, while spectral methods have global support. But wavelets appear to combine the advantages of both spectral and finite-difference bases. One can expect that numerical methods based on wavelets will attain both good spatial and spectral resolution, i.e., the key idea behind the wavelet decomposition is to represent a function in terms of basis functions, called wavelets, which are localized in both space and scale.[13] Moreover, the grid adaptation is achieved by retaining only those wavelets whose coefficients are greater than a given threshold (ϵ). Thus, high resolution computations can be carried out only in those regions where sharp transitions occur. Furthermore, the computational cost of the algorithm is independent of the dimensionality of the problem. Again wavelet methods for PDEs may be divided into two classes: adaptive wavelet-Galerkin method and adaptive wavelet collocation method.

The major difference between these two methods is that wavelet-Galerkin method solve problems in wavelet coefficient space, which one can be considered grid less methods, but wavelet-collocation method solve problem in physical space on a dynamically adaptive grid. Two difficulties associated with wavelet-Galerkin method are the treatment of nonlinearities and general boundary conditions, although different possibilities of dealing with these problems have been proposed.[10] On the other hand, wavelet collocation method do not have these difficulties and the treatment of nonlinearities and general boundary conditions is a relatively straightforward task. Therefore, the aim of this paper is to apply

adaptive wavelet method for solving nonlinear Schrodinger equation (NLSE) on collocation points, which is defined by

$$iu_t(p,t) + \Delta u(p,t) + C_1|u(p,t)|^2 u(p,t) = 0, \tag{1}$$

where Δ is the Laplace-Beltrami operator, $u(p,t)$ is a complex function, $t \geq 0$, p is the point of the general manifold, and C_1 is a constant.

In the current work, we use two different approaches to find the solution of Eq. (1) on different manifolds. In first approach, a dynamic adaptive wavelet method to solve one-dimensional and two-dimensional Schrodinger equation, that is based on Daubechies wavelet with finite difference method on an arbitrary grid. In second approach, a dynamic adaptive wavelet method to solve spherical Schrodinger equation, which is based on spherical wavelet over an optimal spherical geodesic grid.[38]

The rest of the paper is organized as follows. In Sec. 2, we introduce the concept of multi-resolution analysis (MRA) and wavelet (Daubechies wavelet and spherical wavelet). Dynamic adaptive wavelet method for one-dimensional Schrodinger equation, two-dimensional Schrodinger equation and spherical Schrodinger equation are discussed in Sec. 3. Section 4 gives the numerical experiment of Schrodinger equation, and conclusion and outlined are in Sec. 5.

2. Introduction to Wavelets

In this section, we briefly recall the wavelet and multi-resolution analysis (MRA) that will be used in other parts of the paper. The gap between wavelets and finite difference schemes may seem very large. However, a very close connection between these two issues has recently been established.[18] Roughly speaking that the term wavelet is used to describe a spatially localized function, means that the wavelet is assumed to have most of its energy contained in a very narrow region of the physical space. We shall restrict ourselves to wavelets with compact support and focus on the family defined by Daubechies[12,14] for one-dimensional and two-dimensional problem and spherical wavelet[28] on optimal spherical geodesic grid.

2.1. *Daubechies wavelets*

The idea of MRA is first introduced by Stephane Mallat[23] and Yves Meyer[26] in the context of wavelet analysis. This is a new and remarkable idea which deals with a general formalism for construction of an orthogonal basis of wavelets. Indeed, MRA is central to all constructions of wavelet basis. Thus, MRA is a formal approach to constructing orthogonal wavelet bases using a definite set of rules and procedures.

A MRA consists of sequence $\{\mathcal{V}^j : j \in \mathbb{Z}\}$ of embedded closed subspace of $L_2(\mathbb{R})$ that satisfy the following axiom[9]:

- $\ldots \subset \mathcal{V}^{-2} \subset \mathcal{V}^{-1} \subset \mathcal{V}^0 \subset \mathcal{V}^1 \subset \mathcal{V}^2 \subset \ldots$,
- $\bigcup_{j=-\infty}^{\infty} \mathcal{V}^j$ is dense in $L_2(\mathbb{R})$, that is, $\overline{\bigcup_{j=-\infty}^{\infty} \mathcal{V}^j} = L_2(\mathbb{R})$,

- $\bigcap_{j=-\infty}^{\infty} \mathcal{V}^j = \{0\}$,
- $u(x) \in \mathcal{V}^j$ if and only if $u(2x) \in \mathcal{V}^{j+1}$ for all $j \in \mathbb{Z}$, there exist a function $\phi \in \mathcal{V}^0$, such that $\{\phi_k^0 = \phi(x-k), k \in \mathbb{Z}\}$ is an orthonormal basis for $\mathcal{V}^0$. That is,

$$\|u\|^2 = \int_{-\infty}^{\infty} |u(x)|^2 dx = \sum_{k=-\infty}^{\infty} |\langle u, \phi_k^0 \rangle|^2, \quad \forall\, f \in V^0, \tag{2}$$

and it is also required that ϕ has unit area, i.e., $\int_{\infty}^{\infty} \phi(x)dx = 1$. Now we define $\mathcal{W}^j$ to be the orthogonal complement of $\mathcal{V}^j$ in $\mathcal{V}^{j+1}$, i.e., $\mathcal{V}^j \perp \mathcal{W}^j$ and

$$\mathcal{V}^{j+1} = \mathcal{V}^j \bigoplus \mathcal{W}^j. \tag{3}$$

There exists a function, which is called a scaling function $\phi(x) \in \mathcal{V}^0$, such that the sequence $\phi_k^j(x) = 2^{j/2}\phi(2^j x - k)$ is an orthonormal basis for $\mathcal{V}^j$ and $\psi_k^j(x) = 2^{j/2}\psi(2^j x - k)$ is orthonormal basis for $\mathcal{W}^j$ where $j, k \in \mathbb{Z}$, j is the dilation parameter and k is the translation parameter. Mathematically, one can introduces at each step j, the subspace $\mathcal{W}^j$, defined as the orthogonal complement of $\mathcal{V}^j$ in $\mathcal{V}^{j+1}$.

Since $\psi_k^j \in \mathcal{W}^j$ it follows that ψ_k^j is an orthogonal to ϕ_k^j because $\phi_k^j \in \mathcal{V}^j$ and $\mathcal{V}^j \perp \mathcal{W}^j$. Also, because all $\mathcal{W}^j$ are mutually orthogonal, it follows that the wavelets are orthogonal across scale. Therefore, we have following relations.

$$\int_{-\infty}^{\infty} \phi_k^j(x)\phi_l^j(x)dx = \delta_{k,l}, \quad \int_{-\infty}^{\infty} \psi_k^i(x)\psi_l^j(x)dx = \delta_{i,j}\delta_{k,l}, \tag{4}$$

$$\int_{-\infty}^{\infty} \phi_i^k(x)\psi_k^l(x)dx = 0, \quad j \geq i, \tag{5}$$

where $i, j, k, l \in \mathbb{Z}$ and $\delta_{k,l}$ is the Kronecker delta defined as

$$\delta_{k,l} = \begin{cases} 0 & \text{if } k \neq l, \\ 1 & \text{if } k = l. \end{cases} \tag{6}$$

Further, since $\mathcal{V}_0 \subset \mathcal{V}_1$, any function in $\mathcal{V}_0$ can be expanded in term of basis function $\mathcal{V}_1$. In particular, $\phi(x) = \phi_0^0(x)$ so

$$\phi(x) = \sum_{k=-\infty}^{\infty} a_k \phi_k^1(x) = \sqrt{2} \sum_{k=-\infty}^{\infty} a_k \phi(2x-k), \tag{7}$$

where $a_k = \int_{-\infty}^{\infty} \phi(x)\phi_k^1(x)dx$. For compactly supported scaling functions only finitely many a_k will be nonzero and we have

$$\phi(x) = \sqrt{2} \sum_{k=0}^{D-1} a_k \phi(2x-k). \tag{8}$$

Equation (8) is fundamental for wavelet theory and it is know as the dilation equation. $a_0, a_2, \ldots, a_{D-1}$ are called filter coefficients. Here D is an even positive integer called the wavelet genus. The scaling function is uniquely characterized by these

coefficients. In analogy to (8) we can write a relation for the basis wavelet ψ. Since $\psi \in W_0$ and $W_0 \subset V_1$ we can expand ψ (called as wavelet equation) as

$$\psi(x) = \sqrt{2} \sum_{k=0}^{D-1} b_k \phi(2x - k), \tag{9}$$

where the filter coefficients are $b_k = \int_{-\infty}^{\infty} \psi(x)\phi_k^1(x)dx$. Although the filter coefficient a_k and b_k are not normally computed as we don't know ϕ and ψ explicitly.[13] However the filter coefficient b_k can expressed in term of a_k, i.e., $b_k = (-1)^k a_{D-1-k}$, where $k = 0, 1, \ldots, D-1$. An example of Daubechies scaling function $\phi(x)$ and wavelet function $\psi(x)$ for $D = 4$ is shown in Figs. 1(a) and 1(b) and respectively. Further, the accuracy is specified by requiring that $\psi(x) = \psi_0^0(x)$ satisfy for all $m = 0, 1, \ldots, M-1$, where $M = \frac{D}{2}$ vanishing moments

$$\int_{-\infty}^{\infty} \psi(x) x^m dx = 0. \tag{10}$$

A function $u \in \mathcal{V}^J$ can be expanded in various ways. For example, there is the pure scaling function expansion

$$u(x) = \sum_{k=-\infty}^{\infty} c_k^J \phi_k^J(x), x \in \mathbb{R}, \tag{11}$$

where $c_k^J = \int_{-\infty}^{\infty} u(x)\phi_k^J(x)dx$, for any $J_0 \leq J$, where J_0 is the coarse level of approximation and J is the finest level of resolution, there is also the wavelet expansion is complete

$$u(x) = \sum_{j=J_0}^{J-1} \sum_{k=-\infty}^{\infty} d_k^j \psi_k^j(x), x \in \mathbb{R}, \tag{12}$$

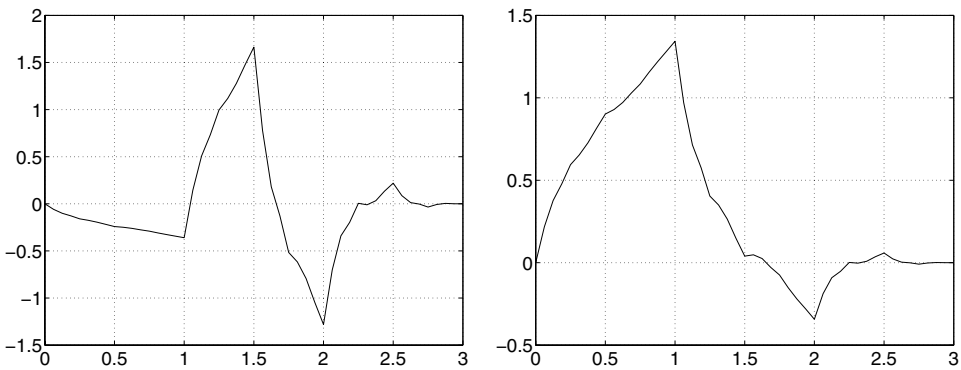

(a) (b)

Fig. 1. (a) Daubechies wavelet $\psi(x)$ and (b) scaling function $\phi(x)$.

where due to orthonormality of the wavelets $d_k^j = \int_{-\infty}^{\infty} u(x)\psi_k^j(x)dx$. Furthermore, the decay of d_k^j depends on the local regularity of $u(x)$ as

$$|d_k^j| \leq C2^{-j(L+1)/2} \max_{\zeta \in [k2^{-j},(k+M-1)2^{-j}]} |u^{(M)}(\zeta)|. \tag{13}$$

From Eq. (13), one can find that if the function $u(x)$ behaves like a polynomial of order less than M in side the small interval, then the coefficients d_k^j vanishes exactly, means one can view the magnitude of d_k^j as a direct measure of how well the assumption of local polynomial behavior, underlying the finite difference scheme, is satisfied. Equation (13) makes the use of wavelets as local error estimators in connection with finite difference methods a natural and efficient approach.

Moreover, if $u^{(M)}$ is differs from zero, the coefficients d_k^j will decay exponentially with respect to the scale parameter j, again also the information given by Eq. (13) provides a local measure of the regularity of the function or rather the closeness to local polynomial behavior. Hence, this is exactly what we utilize to determine the need for order and/or mesh adjustments.

2.2. *Spherical wavelets*

To construct an spherical geodesic grid (also called icosahedral-hexagonal grid), we begin with a platonic solid (see Fig. 2), which has spherical triangular faces, then with help of subdivision scheme one can get new vertices onto the surface of the sphere. We will consider the icosahedral subdivision for which $\#\mathcal{K}^j = 10 \times 4^j + 2$ at subdivision level j. For each of $\mathcal{K}^j$ grid points is surrounded by 6 nearest neighbors except for the original 12 icosahedral vertices means our platonic solid. Let $\mathcal{S}$ be a triangulation of the sphere S and denote the set of all vertices obtained after subdivisions with $\mathcal{S}^j = \{p_k^j \in S | k \in \mathcal{K}^j\}$, where $\mathcal{K}^j$ is an index set, and let q_k^j be the center of the triangle p_i^j, p_k^j, p_{k+1}^j (see Fig. 3). Since $\mathcal{S}^j \subset \mathcal{S}^{j+1}$ we also let $\mathcal{K}^j \subset \mathcal{K}^{j+1}$. Let $\mathcal{M}^j = \mathcal{K}^{j+1}/\mathcal{K}^j$ be the indices of the vertices added when going from level j to $j+1$.

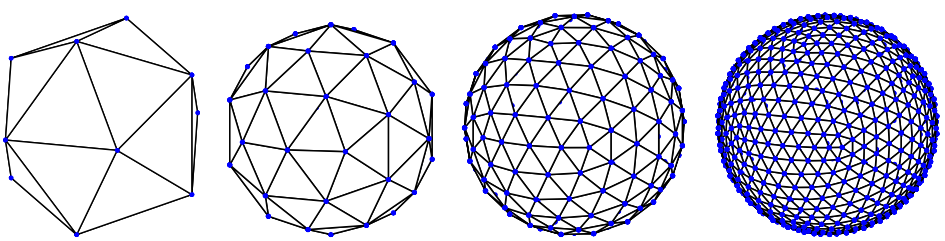

(a) level 0 (b) level 1 (c) level 1 (d) level 1

Fig. 2. Geodesic grid generation based on an icosahedron embedded in the sphere.

A second generation MRA[33] of the sphere provides a sequence $\mathcal{V}^j \subset L_2(S)$ with $j \geq 0$ and the sphere $S = \{p = (p_x, p_y, p_z) \in \mathbb{R}^3 : \|p\| = a\}$, where a is the radius of the sphere.

- $\mathcal{V}^j \subset \mathcal{V}^{j+1}$,
- $\bigcup_{j\geq 0} \mathcal{V}^j$ is dense in $L_2(S)$,
- Each $\mathcal{V}^j$ has a Riesz basis of scaling functions $\{\phi_k^j \mid k \in \mathcal{K}^j\}$.

Since $\phi_k^j \in \mathcal{V}^j \subset \mathcal{V}^{j+1}$, for every scaling function ϕ_k^j filter coefficients $h_{k,l}^j$ exists such that

$$\phi_k^j = \sum_{l\in\mathcal{K}^{j+1}} h_{k,l}^j \phi_l^{j+1}. \tag{14}$$

Note that the filter coefficients $h_{k,l}^j$ can be different for every $k \in \mathcal{K}^j$ at a given level $j \geq 0$. Therefore each scaling function satisfies a different refinement relation. Each MRA is accompanied by a dual MRA consisting of nested spaces $\tilde{V}^j$ with bases by the dual scaling functions $\tilde{\phi}_k^j$, which are biorthogonal to the scaling functions:

$$\langle \phi_k^j, \tilde{\phi}_{k'}^j \rangle = \delta_{k,k'}, \quad \text{for } k, k' \in \mathcal{K}^j, \tag{15}$$

where $\langle f, g\rangle = \int_s fg dw$ is the inner product on the sphere. The dual scaling functions satisfy refinement relations with coefficients $\{\tilde{h}_{k,l}^j\}$.

One most important thing when you are going to build MRA to construction of wavelets. They encode the difference between two successive levels of representation, that is there from Riesz basis for the space $\mathcal{W}$, which is complement of $\mathcal{V}^j$ in $\mathcal{V}^{j+1}$ (i.e., $\mathcal{V}^{j+1} = \mathcal{V}^j \bigoplus \mathcal{W}^j$). The construction of the wavelets form a Riesz basis for $L^2(S)$ and allow a function to be represented by its wavelet coefficients. Since $\mathcal{W}^j \subset \mathcal{V}^{j+1}$, we can write

$$\psi_k^j = \sum_{l\in\mathcal{K}^{j+1}} g_{k,l}^j \phi_l^{j+1}, \tag{16}$$

and the spherical wavelets ψ_m^j have $\tilde{d}$ vanishing moments, if $\tilde{d}$ is the independent polynomials $P_i, 0 \leq i \leq \tilde{d}$ exist such that

$$\langle \psi_m^j, P_i \rangle = 0 \quad \forall\, j \geq 0,\ m \in \mathcal{M}^j, \tag{17}$$

where $\mathcal{M}^j$ is the index set and polynomial P_i are define as the restriction to the sphere of polynomials on $\mathbb{R}^3$.

Consider a function $u(p) \in L_2(S)$ which can be approximated as

$$u(p) = \sum_{k\in\mathcal{K}^0} c_k^0 \phi_k^0(p) + \sum_{j=0}^{\infty} \sum_{m\in\mathcal{M}^j} d_m^j \psi_m^j(p). \tag{18}$$

This equation can be written as sum of two terms composed of wavelets whose amplitudes are, above and below some prescribed threshold ϵ that is

$$u(p) = u_{\geq}(p) + u_{<}(p), \tag{19}$$

where

$$u_{\geq}(p) = \sum_{k \in \mathcal{K}^0} c_k^{J_0} \phi_k^{J_0}(p) + \sum_{j=J_0}^{\infty} \sum_{\substack{m \in \mathcal{M}^j \\ |d_m^j| \geq \epsilon}} d_m^j \psi_m^j(p), \tag{20}$$

$$u_{<}(p) = \sum_{j=J_0}^{\infty} \sum_{\substack{m \in \mathcal{M}^j \\ |d_m^j| < \epsilon}} d_m^j \psi_m^j(p), \tag{21}$$

where J_0 is the coarse level of approximation, Donoho[15] has shown that for smooth enough u,

$$\|u(p) - u_{\geq}(p)\|_{\infty} \leq c_1 \epsilon, \tag{22}$$

and the number of significant coefficients $N(\epsilon) = \mathcal{N}$ depends on ϵ,

$$N(\epsilon) \leq c_2 \epsilon^{-n/d}, \tag{23}$$

where d is the order of interpolation, n is the dimension of the problem and the coefficients c_i's depend on the function. Combining relations (22) and (23) gives the following bound on the error in terms of $N(\epsilon)$

$$\|u(p) - u_{\geq}(p)\|_{\infty} \leq c_3 N(\epsilon)^{-d/n}. \tag{24}$$

Note that d controls the number of zero moments of the interpolating scaling function. This error estimate is consistent with numerical experiment for flat geometry (Vasilyev and Bowman[34,35]), and on the sphere (Mehra and Kevlahan[24]). Further, different error estimate is consistent with numerical experiment for the multiscale differential operators on sphere in Refs. 4 and 5.

In order to realize the benefits of the wavelet compression, we need to have the ability to reconstruct $u_{\geq}(p)$ from the subset of $N(\epsilon) \subset N$ of significants grid points. Furthermore, we recall that every wavelet $\psi_l^j(x)$ is uniquely associated with a collocation point. Hence once the wavelet decomposition is performed, each grid point is uniquely associated either with the wavelet or scaling function at the coarsest level of resolution. Consequently, the collocation point should be omitted from the computational grid, if the associated wavelet is omitted from the approximation. This procedure results in a set of nested adaptive computational grids $\mathcal{S}_{\geq}^j \subset \mathcal{S}^j$, such that $\mathcal{S}_{\geq}^j \subset \mathcal{S}_{\geq}^{j+1}$, for any $j < J-1$, where J is the finest level of resolution present in approximation $u_{\geq}(x)$ (for detail see in one dimensional and multi dimensional[34,35] and on the sphere[24]). Thus, if there are no points in the immediate vicinity of a grid point p_i^j, means $|d_k^j| \leq \epsilon$ for all $k \in N(i)$, and the points $p_k^{j+1}, k \in N(i)$, are not

present in $\mathcal{S}^{j+1}$, then there exists some neighborhood Ω_i^j of p_i^j, where the function can be interpolated by a wavelet interpolant based on $s_{k,m}^j (k \in \mathcal{K}_m)$.

$$\left| u(p) - \sum_{k \in \mathcal{K}(i)} s_{k,m}^j \phi_k^j(p) \right| \leq c_3 \epsilon, \tag{25}$$

where the coefficients $s_{k,m}^j$ can be chosen according as Ref. 24.

When solving the evolution equations an additional criterion for grid adaptation should be added. The computational grid should consist of grid points associated with wavelets whose coefficients are significant or could become significant during a time step. In other words, at any instant in time, the computational grid should include points associated with wavelets belonging to an adjacent zone of wavelets for which the magnitude of their coefficients is greater than an *a priori* prescribed threshold.

3. Dynamic Adaptive Wavelet Method

Wavelet method is a natural tool for grid adaptation. The strength of a dynamic adaptive wavelet method now appears. For functions which contain isolated small scales on a large-scale background, most wavelet coefficients are small, thus we retain a good approximation even after discarding a large number of wavelets with small coefficients. The accuracy in the adaptive wavelet method depends upon the threshold parameter ϵ. Furthermore, to capture the singular effects in the solution of Schrodinger equation by using classical discretizations based on uniform (or even quasi-uniform) partitions into grid would require a very fine resolution near the singularities and thus lead to enormous problem sizes. One can see that the nature of the solution begs for the use of adaptive methods which would give finer resolution in the regions of shock discontinuities and maintain coarser resolution otherwise.

3.1. *One-dimensional nonlinear Schrodinger equation*

Consider a periodic function u in the range $[-L/2, L/2]$, then Eq. (1) can be written as

$$\begin{aligned} u_t(x,t) &= -i\Delta u(x,t) - iC_1|u(x,t)|^2 u(x,t) \\ u(x,0) &= h(x) \\ u(x,t) &= u(x+L,t), \end{aligned} \tag{26}$$

where $t \geq 0$ and $x \in [-L/2, L/2]$, and $\Delta = \frac{\partial^2}{\partial x^2}$,

Again consider $N = 2^J$ and defined a grid consisting of the points

$$x_l^J = \left(\frac{l}{N} - \frac{1}{2} \right) L, \quad l = 0, 1, 2, \ldots, N-1. \tag{27}$$

Define a vector $\mathbf{u}$(t) such that

$$u_l^J(t) = u^J(x_l, t), \quad l = 0, 1, 2, \ldots, N-1, \tag{28}$$

where $u^J(x,t)$ is an approximate solution of Eq. (26) of the form Eq. (11). Hence the finite differentiation matrix

$$\frac{d}{dt}\mathbf{u}(t) = \mathbf{L}\mathbf{u}(t) + \mathbf{N}(\mathbf{u}(t))\mathbf{u}(t), t \geq 0 \tag{29}$$

$$\mathbf{u}(0) = \mathbf{h} = [h(x_0), h(x_1), h(x_2), \ldots, h(x_{N-1})]^T, \tag{30}$$

where

$$\mathbf{L} = \frac{-i}{2}\beta\frac{\mathbf{D}_p^{(2)}}{L^2} \tag{31}$$

$$\mathbf{N}(\mathbf{u}(t)) = i\gamma\text{diag}(|u_t(t)|^2, l = 0, 1, \ldots, N-1). \tag{32}$$

Interpolation with algebraic polynomials is the most common and popular way to generate differencing coefficients. One simply fits the polynomial to the data, followed by differentiation of the polynomial, and finally one evaluates the polynomial at the point of interest. Since we are using grid point from the wavelet, derivatives on uniform or nonuniform grid are approximated using Lagrangian interpolating polynomial through p points.[19] We consider only odd $p \geq 3$ because it makes the algorithm simpler. Let $w = \frac{p-1}{2}$ and define

$$u_I(x) = \sum_{k=i-w}^{i+w} u(x_k)\frac{P_{w,i,k}(x)}{P_{w,i,k}(x_k)}, \tag{33}$$

where

$$P_{w,i,k}(x) = \prod_{\substack{l=i-w \\ l\neq k}}^{i+w} (x - x_l). \tag{34}$$

Equation (33) implies that u_I interpolates u at the grid points, i.e $u_I(x_i) = u(x_i)$ for $i = 0, 1, 2, \ldots, N_J - 1, N_J$. Differentiation of $u_I(x)d$ times yields

$$u_I^{(d)}(x) = \sum_{k=i-w}^{i+w} u(x_k)\frac{P_{w,i,k}^{(d)}(x)}{P_{w,i,k}(x_k)}. \tag{35}$$

The derivatives $u_I^{(d)}(x)$ can be approximated at all grid points by

$$u_I^{(d)}(x) = \mathcal{D}_p^{(d)}u, \tag{36}$$

where differentiation matrix $\mathcal{D}_p^{(d)}u$ is defined by

$$[\mathcal{D}_p^{(d)}]_{i,k} = \frac{P_{w,i,k}^{(d)}(x_i)}{P_{w,i,k}(x_k)}; \quad d = 1, 2. \tag{37}$$

The first and second derivatives are

$$P^{(1)}_{w,i,k}(x) = \sum_{\substack{l=i-w \\ l\neq k}}^{i+w} \prod_{\substack{m=i-w \\ m\neq k,l}}^{i+w} (x - x_m), \tag{38}$$

$$P^{(2)}_{w,i,k}(x) = \sum_{\substack{l=i-w \\ l\neq k}}^{i+w} \sum_{\substack{m=i-w \\ m\neq k,l}}^{i+w} \prod_{\substack{n=i-w \\ n\neq k,l}}^{i+w} (x - x_n). \tag{39}$$

Now Eq. (29) can be approximated using Crank-Nicolson method

$$\frac{\mathbf{u}(t+\Delta t) - \mathbf{u}(t)}{\Delta t} = \mathbf{L}\frac{\mathbf{u}(t+\Delta t) - \mathbf{u}(t)}{2} + \mathbf{N}\left(\frac{\mathbf{u}(t+\Delta t) - \mathbf{u}(t)}{2}\right)\frac{\mathbf{u}(t+\Delta t) - \mathbf{u}(t)}{2} \tag{40}$$

and we obtain the time stepping procedure we can get

$$\mathbf{A}\mathbf{u}_{n+1} = \mathbf{B}\mathbf{u}_n + \Delta t\mathbf{N}\left(\frac{\mathbf{u}_{n+1} + \mathbf{u_n}}{2}\right)\frac{\mathbf{u}_{n+1} + \mathbf{u_n}}{2}, \quad n = 0, 1, 2, \ldots, n_1 - 1 \tag{41}$$

$$\mathbf{u}_0 = \mathbf{h}, \tag{42}$$

where

$$\mathbf{A} = \mathbf{I} - \frac{\delta}{2}\mathbf{L} \tag{43}$$

$$\mathbf{B} = \mathbf{I} + \frac{\delta}{2}\mathbf{L} \tag{44}$$

$$\mathbf{u}_n = \mathbf{u}(n\Delta t). \tag{45}$$

Consider $u(x^J_k, t), k = 0, 1, \ldots, N-1$ be the approximate solution of $u(t)$. The success of an adaptive method relies on a procedure for determining a grid which is dense where u is erratic and sparse where u is smooth. In the above estimate (13), the error at $k/2^j$ dependent on size of the neighboring intervals, and a large value of $|d^j_k|$ is an indication that the grid spacing $1/2^j$ is too coarse to resolve u properly in the interval I^j_k. Hence when a large value of $|d^j_k|$ arises, one can add point with spacing $1/2^{j+1}$ about the position $k/2^j$ to reduce the error locally. In Ref. 19 it is suggested that only a few points be added at location $k/2^j$. However, above mentioned estimates shows that it is reasonable to distribute points evenly over enter interval I^j_k because the large gradient can be located anywhere with in the support of the corresponding wavelet. Hence, if the solution vector u is define for a course grid, then interpolate to the values on the fine grid and compute d^j_k. The

basic steps are presented in Algorithm — (1).

Algorithm 1: Grid adaptation for solving one-dimensional Schrodinger equation.

while *time* $\leq$ *final time* **do**
  After solving the given problem on a uniform grid for the initial solution profile. Apply the discrete wavelet transform to the solution profile and calculate the wavelet coefficient. The wavelet coefficient will be smaller where the solution is smooth and large at the place singularity.
  Remove the grid points where $|d_k^j| < \epsilon$ (prescribed threshold) and keep the remaining grid points.
  Then apply Lagrange finite difference on a irregular grid on a remaining grid points and get next step solution,
end

3.2. *Two-dimensional nonlinear Schrodinger equation*

Detecting singularity in two-dimensional domain is more complex than detecting singularity on one-dimensional domain. It is critical to ensure that the grid selection mechanism does not miss anything in the domain. Here, we have explained two-dimensional adaptive wavelet method, let us consider $p = (x, y)$ is a point on a square bounded domain then Eq. (1) can be written as

$$iu_t(x, y, t) + \Delta u(x, y, t) + C_1|u(x, y, t)|^2 u(x, y, t) = 0, \tag{46}$$

where Δ is the Laplacian operator. But u is the unknown scalar function defined on a square bounded domain with periodic boundary conditions. The time discretization goes similarly as in the one-dimensional case. The two-dimensional grid selection mechanism used here is fundamentally the one-dimensional wavelet grid selection mechanism explained above applied in a tensor product manner.[8] After space discretization the matrices $\mathbf{A}$ and $\mathbf{B}$ computational cost will be $N^2 \times N^2$ that is very large computational cost for practical purpose, however for a $N \times N$ in one-dimensional case, to overcome this problem, and take full advantage of tensorial wavelet based one can factorized approximation of two-dimensional operators. The use of Alternated Direction Implicit (ADI) methods,[36] to approximate the two dimensional operator $(Id - \alpha\Delta)$ by product of one-dimensional operators

$$(Id - \alpha\Delta) = \left(Id - \alpha\frac{\partial^2}{\partial x^2}\right)\left(Id - \alpha\frac{\partial^2}{\partial y^2}\right) \quad \text{for small } \alpha, \tag{47}$$

with this factorization, matrices $\mathbf{A}$ and $\mathbf{B}$ for the second-order Crank-Nicolson method scheme is

$$\mathbf{A} = \left(\mathbf{I} - \gamma\frac{\delta t}{2}\frac{\partial^2}{\partial x^2}\right)\left(\mathbf{I} - \gamma\frac{\delta t}{2}\frac{\partial^2}{\partial y^2}\right) \tag{48}$$

$$\mathbf{B} = \left(\mathbf{I} + \gamma\frac{\delta t}{2}\frac{\partial^2}{\partial x^2}\right)\left(\mathbf{I} + \gamma\frac{\delta t}{2}\frac{\partial^2}{\partial y^2}\right). \tag{49}$$

The basic steps are presented in Algorithm — (2).

Algorithm 2: Grid adaptation for solving two-dimensional Schrodinger equation.

while *time* $\leq$ *final time* **do**
  After solving the given problem on a uniform grid for the initial solution profile. Apply the one-dimensional discrete wavelet transform of the rows followed by one-dimensional discrete wavelet transform of the column to the solution profile and calculate the wavelet coefficient. The wavelet coefficient will be smaller where the solution is smooth and large at the place singularity.
  Remove the grid points where $|d_k^j| < \epsilon$ (prescribed threshold) and keep the remaining grid points.
  Then apply Lagrange finite difference on a irregular grid both rows and columns on a remaining grid points and get next step solution,
end

3.3. *Schrodinger equation on the sphere*

In this section, we will discuss spherical Schrodinger equation over adaptive optimal spherical geodesic grid[38] with help of spherical wavelet. Since $S = \{p = (x, y, z) \in \mathbb{R}^3 : x, y, z \in \mathbb{R} \text{ and } \|p\| = a\}$, where a is the radius of the sphere. Then Eq. (1) can be written as

$$iu_t(p,t) = -\Delta u(p,t) - C_1|u(p,t)|^2 u(p,t). \tag{50}$$

We can write numerical approximation of the Laplace-Beltrami operator on the sphere Δ[25] is

$$\Delta u(p_i^j) = \frac{1}{A_s(p_i^j)} \sum_{k \in N(i)} \frac{\cot \alpha_{i,k} + \cot \beta_{i,k}}{2} [u(p_k^j) - u(p_i^j)],$$

where p_i^j be a vertex of the triangulation at resolution j and $p_k^j, k \in N(i)$ is the neighboring vertices around p_i^j, $\alpha_{i,k}$ and $\beta_{i,k}$ are the angles in a Fig. 3 and $N(i)$ is the set of nearest vertices of the vertex p_i^j, and $A_s(p_i^j)$ is the area of the one ring neighborhood given by

$$A_s(p_i^j) = \frac{1}{8} \sum_{k \in N(i)} (\cot \alpha_{i,k} + \cot \beta_{i,k}) \|p_k^j - p_i^j\|^2.$$

Since approximation of Laplace-Beltrami operator on the sphere plays a vital role in solving Schrodinger equation on the sphere. The convergence of Laplace-Beltrami operator on an spherical geodesic grid and optimal spherical geodesic grid is discussed in Refs. 24, 25 and 38. Although the approximation of Laplace-Beltrami operator on the spherical geodesic grid has been used in practice but it suffers couple of drawbacks (i.e., truncation error is quite large). Which can be removed

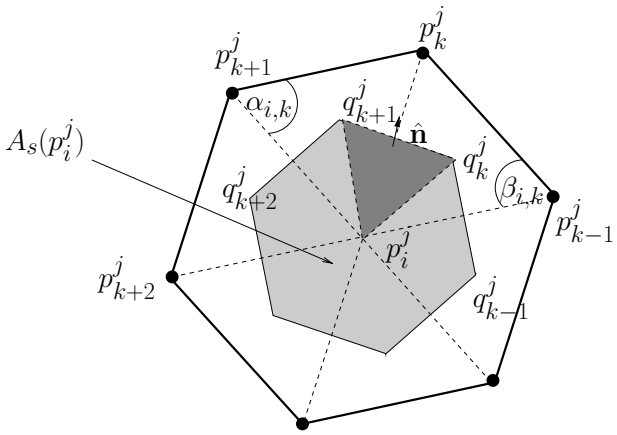

Fig. 3. Schematic figure of angles $\alpha_{i,k}, \beta_{i,k}$, where $\alpha_{i,k}, \beta_{i,k}$ are angle of $p^j_i p^j_{k+1} p^j_k$ and $p^j_i p^j_{k-1} p^j_k$ are respectively. Further, $\hat{\mathbf{n}}$ is the unit normal vector to an edge $q^j_k q^j_{k+1}$.

in the approximation of Laplace-Beltrami operator on optimal spherical geodesic grid up to some extent.[24] Here we refer as dynamically adaptive in the sense that the irregular optimal geodesic grid of collocation points is dynamically adapted in time and follows the local structure that appear in the solution. The necessary steps to construct a dynamically adaptive algorithm for the solution of Schrodinger equation on an optimal spherical geodesic grid is as described in Algorithm — (3).

Algorithm 3: Grid adaptation for solving Schrodinger equation on the sphere.

1 **while** *time* $\leq$ *final time* **do**
2 After getting the solution $u_{\geq}(t)$ on the adaptive grid, compute the values of wavelet coefficients corresponding to each component of the solution using the fast wavelet transform. For a given threshold ϵ we update $s^{t+\Delta t}_{\geq}$ based on the magnitude of wavelet coefficients. We also add an adjacent zone to the significant coefficients to allow for the change in the solution during one time step, as described in Section 2.2.
3 If there is no change between computational grids $S^t_{\geq}$ and $S^{t+\Delta t}_{\geq}$, we go directly to next step. Otherwise we interpolate the values of the solution at the collocation points $S^{t+\Delta t}_{\geq}$, which are not included in $S^t_{\geq}$.
4 We integrate the resulting system of ordinary differential equations in time to obtain new values $u_{\geq}(t + \Delta t)$ at positions on adaptive grid $S^{t+\Delta t}_{\geq}$, and go back to step 2 find the solution $u_{\geq}(t)$ on the adaptive grid.
5 **end**

With such an algorithm the grid of collocation points adapts dynamically in time to follow local structures that appear in the solution. Moreover by omitting

wavelets with coefficients below a threshold parameter, we automatically control the L_∞ — norm error of approximation. Thus the method has another important feature: active control of the accuracy of the solution.

4. Numerical Results and Discussion

In this section, numerical simulations are made for the one-dimensional, two-dimensional and spherical Schrodinger equation to illustrate the effectiveness of the proposed methods. The dynamic adaptive wavelet method is used to resolve rapid and localized variations in the solution of Schrodinger equation.

4.1. *One-dimensional Schrodinger equation*

To solve one-dimensional Schrodinger equation (Eq. (26)), we consider a periodic function $u(x,0) = 2\text{sech}(x)$, $u \in [-L/2, L/2]$, where $L = 64$. The parameters of Eq. (26) are $C_1 = 2$ and $h(x) = 2\text{sech}(x)$. The numerical parameters are $J = 10$ (making $N = 1024$), $\epsilon = 10^{-4}$, $p = 5, \Delta t = 1/2^{10}$, and $D = 16$ (wavelets genus). The initial solution ($t = 0$) and its adaptive grid are plotted in left of Fig. (4), and the solution at time $t = 0.5$ and its adaptive grid are ploted in right of Fig. 4. We observed from Fig. (4), that the grid becomes more dense near the singularity.

In order to demonstrate the tremendous savings of the adaptive algorithm, we need to compare the number of grid points used in the adaptive and nonadaptive methods. That can be computed by the compression coefficient $C = N(\epsilon = 0)/N(\epsilon)$. The larger the compression coefficient, the more efficient the adaptive algorithm. In Fig. 5 (left) it is clear that hight compression coefficient obtained at $\epsilon = 10^{-1}$, furthermore this figure say that when ϵ goes to zero means the compression coefficient goes to one, i.e., adaptive algorithm becomes nonadaptive. In Fig. 5 (right) we have computed error with different ϵ. The advantage of adaptive wavelet method

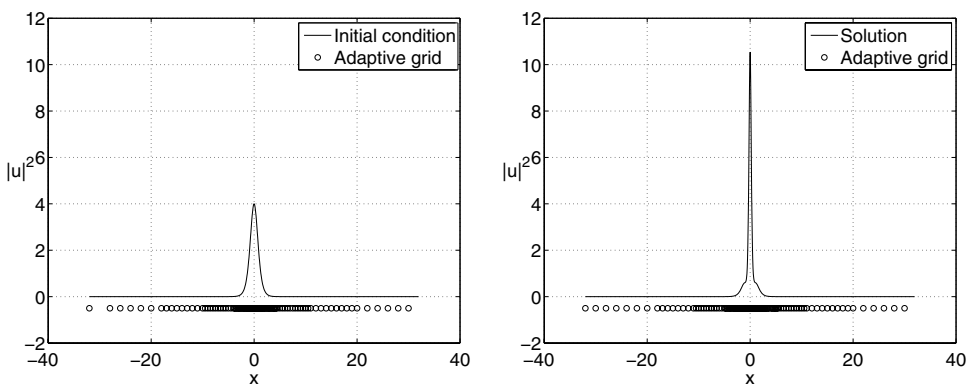

Fig. 4. Solution of one-dimensional Schrodinger equation at time $t = 0.5$.

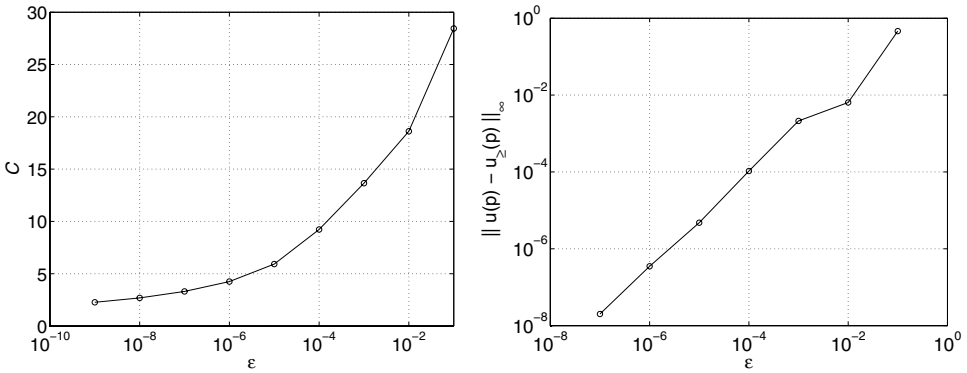

Fig. 5. Compression coefficient with different ϵ for initial condition (left) and error with ϵ (right).

is to detect the regions of the computational domain which contain small singular region as mentioned in Fig. 4.

4.2. *Two-dimensional Schrodinger equation*

In two-dimensional Schrodinger equation (Eq. (46)), we choose a initial condition[39] $u(x, y, t = 0) = (1 + \sin(x))(2 + \sin(y))$ on the square domain $[-L/2, L/2] \times [-L/2, L/2]$, where $L = 8$.

Here we have plotted initial condition in Fig. 6 (left) and its adaptive grid in Fig. 6 (right). The problem is solved till time $t = 0.11$, and the solution and its adaptive grid are plotted in Fig. 7. here we also observed from Fig. (6) (right) and Fig. 7 (right), that the grid becomes more dense near the singularity.

We have plotted compression coefficient with different ϵ in the left of the Fig. 8. In Fig. 8 (right) we have plotted compression coefficient at different time. Where the compression coefficient decreases with increasing singularity. Figure 9 clearly

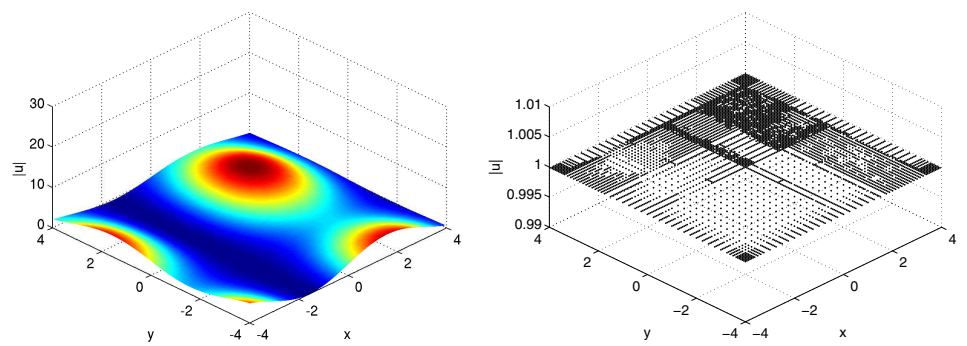

(a) (b)

Fig. 6. (a) Initial condition of two-dimensional Schrodinger equation, (b) and its adaptive grid.

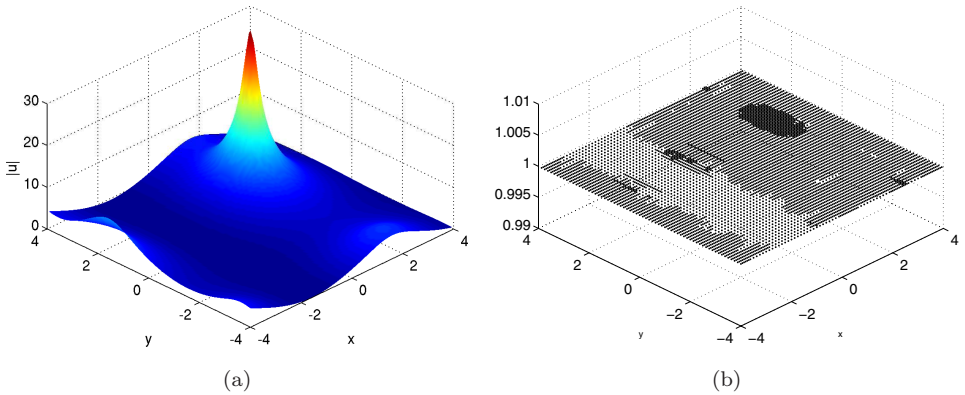

(a) (b)

Fig. 7. (a) The solution of two-dimensional Schrodinger equation time $t = 0.11$, (b) and its adaptive grid.

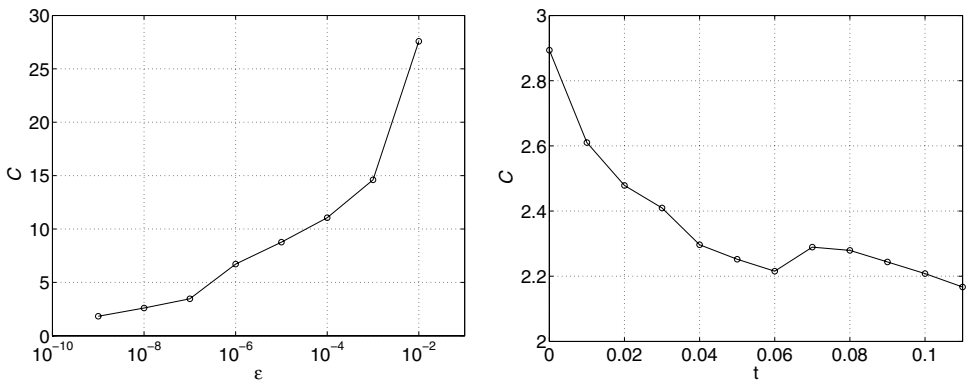

Fig. 8. Relation between compression coefficient with ϵ, (see left side) and compression coefficient with time (see right side) for two-dimensional Schrodinger equation.

demonstrates the convergence of the numerical method with the decreasing ϵ. Thus prescribing the value of ϵ, we can actively control the accuracy of the solution.

4.3. *Schrodinger equation on the sphere*

For the testing nonlinear Schrodinger equation on the sphere, we take initial condition which is a simple complex Gaussian function on the sphere given by

$$u(\theta, \phi, t = 0) = 2 \exp\left[-i\frac{(\theta - \theta_0) + (\phi - \phi_0)}{L^2 * (t + 1)}\right] \exp\left[-\frac{(\theta - \theta_0)^2 + (\phi - \phi_0)^2}{L^2 * (t + 1)}\right], \quad (51)$$

where θ $(-\pi \leq \theta \leq \pi)$ and ϕ $(-\pi/2 \leq \phi \leq \pi/2)$ are the longitude and latitude respectively. $\theta_0 = 0$, $\phi_0 = 0$, $L = 1/2\pi$ and $C_1 = 1$.

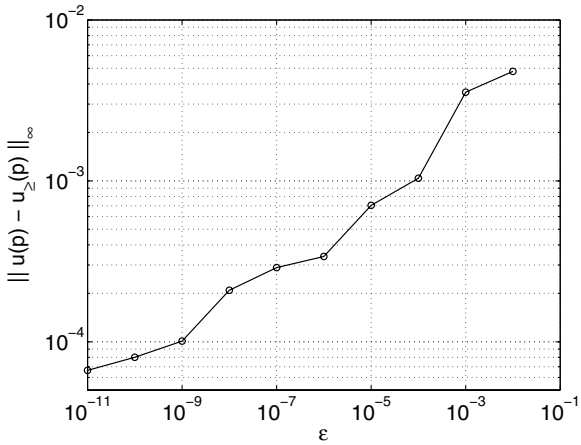

Fig. 9. Relation between ϵ and error for the solution of two-dimensional Schrodinger equation.

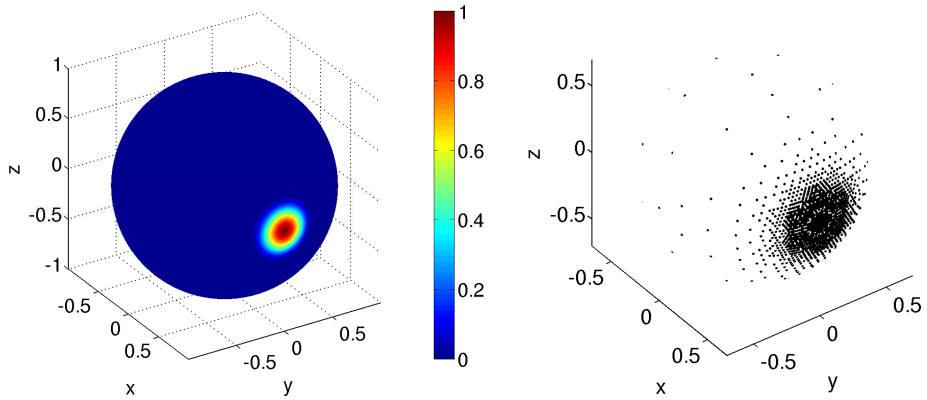

Fig. 10. The initial test function (51) with $\theta_0 = 0$, $\phi_0 = 0$ and $L = 1/2\pi$(left), and its adaptive grid with $\epsilon = 10^{-4}$.

In Fig. 10 (left) and (right), we have plotted initial condition (Eq. (51)) and the dynamic adaptation of the computational grid respectively. Moreover, one can observe from Fig. 11 (left) that a compression coefficient $C \approx 10^2$ for $\epsilon \approx 10^{-4}$. Next we study the convergence of the dynamic adaptive wavelet method on the Schrodinger equation. We emphasize that the convergence study for the adaptive wavelet algorithms with $\epsilon \neq 0$ should be distinguished from the refinement computational grid. i.e., increasing the maximum allowable level of resolution J. In Fig. 11 (right), the maximum allowable level of resolution is $J = 7$ fixed. It means beyond that label $J = 7$ their is no change in $N(\epsilon)$.

For an initial condition Eq. (51), we have plotted relation between ϵ and error in Fig. 12 (left). Moreover we have also plotted relation (24) between $N(\epsilon)$, and

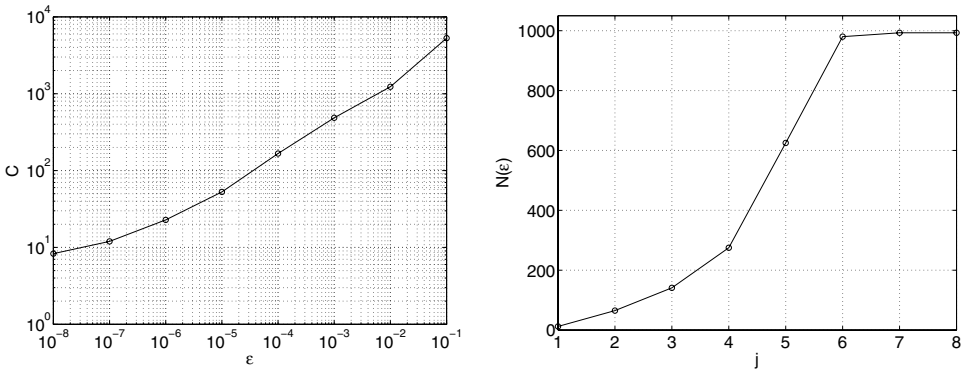

Fig. 11. Relation between compression coefficient ($\mathcal{C}$) and ϵ of the function 51 (left), and $N(\epsilon)$ as a function of number of allowed levels j (right).

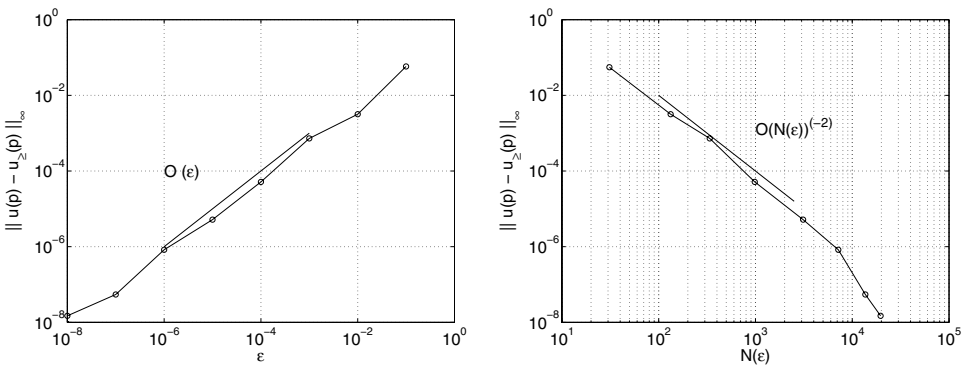

Fig. 12. Relation between $||u(p) - u_{\geq}(p)||_{\infty}$ and ϵ (left), and relation between $||u(p) - u_{\geq}(p)||_{\infty}$ and $N(\epsilon)$ (right).

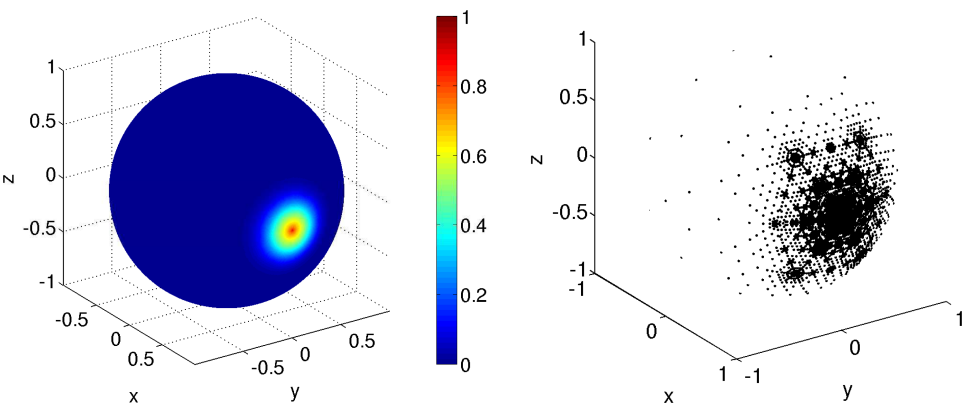

Fig. 13. The solution and dynamically adapted grid for the nonlinear Schrodinger equation at time $t = 0.1$ with tolerance $\epsilon = 10^{-4}$.

error (which is $O(N(\epsilon)^{-2})$ from Fig. 12 (right) as we take butterfly interpolation (i.e., $d = 4$). Conclusively, the error is controlled by ϵ. In Eq. (50), it is expected that the solution of nonlinear Schrodinger equation slowly disperses with passing of time. This equation is solved till time $t = 0.1$, and the solution and its adaptive grid for $\epsilon = 10^{-4}$ are plotted in Fig. 13 respectively.

5. Conclusion and Future Direction

In this work, we have demonstrated how a dynamic adaptive wavelet method works with local singularity of the solution of Schrodinger equation in a simple manner. The wavelet decomposition is used for grid adaption and interpolation, while hierarchical finite difference scheme is apply for grid discretization of Laplace-Beltrami operators. The results indicate that the computational grid and associated wavelets can very efficiently adapt to the local irregularities of the solution in order to resolve sharp transition regions. The proposed dynamic adaptive wavelet method can be extended to other type of partial differential equations on the sphere with discontinuous solutions, moreover one can extend the adaptive wavelet method to other complex geometries leaving freedom and flexibility to choose the wavelet basis depending on the application.

Acknowledgment

This research work was supported by Department of Science and Technology, India, under the Grant No. RP02417.

References

1. X. Antoine, C. Besse and S. Descombes, Artificial boundary conditions for one-dimensional cubic nonlinear schrodinger equations, *SIAM J. Numer. Anal.* **43** (2006) 2272–2293.
2. X. Antoine, E. Lorin, J. Sater, F. Fillion-Gourdeau and A. D. Bandrauk, Absorbing boundary conditions for relativistic quantum mechanics equations, *J. Comput. Phys.* **277** (2014) 268–304.
3. A. Arnold, Numerically absorbing boundary conditions for quantum evolution equations, *VLSI Design* **6** (1998) 313–319.
4. R. Behera and M. Mehra, Integration of barotrophic vorticity equation over spherical geodesic grid using multilevel adaptive wavelet collocation method, *Appl. Math. Modelling* **37** (2013) 5215–5226.
5. R. Behera, M. Mehra and N. K. R. Kevlahan, Multilevel approximation of the gradient operator on an adaptive spherical geodesic grid, *Adv. Comput. Math.* (2014) 1–27.
6. R. M. Caplan and R. Carretero-Gonzalez, A modulus-squared dirichlet boundary condition for time-dependent complex partial differential equations and its application to the nonlinear Schrodinger equation, *SIAM J. Sci. Comput.* **36** (2014) A1–A19.
7. C. Cerjan and K. Kulander, Efficient time propagation for finite-difference representations of the time dependent Schrodinger equation, *Comput. Phys. Comm.* **63** (1991) 529–537.

8. P. Charton and V. Perrier, A pseudo-wavelet scheme for the two-dimensional Navier-Stokes equations, *Comp. Appl. Math.* **15** (1996) 139–160.
9. C. K. Chui, *An Introduction to Wavelets*, Academic Press, Boston, MA, 1992.
10. A. Cohen and I. Daubechies, Wavelets on the interval and fast wavelet transforms, *Appl. Comput. Harmon. Anal.* **1** (1993) 5481. *Constr. Appro.* **5**.
11. C. E. Dateo and H. Metiu, Numerical solution of the time dependent Schrodinger equation in spherical coordinates by Fourier transform methods, *J. Chem. Phys.* **95** (1991) 7392–7400.
12. I. Daubechies, Orthonormal bases of compactly supported wavelets, *Comm. Pure Appl. Math.* **41** (1988) 499–519.
13. I. Daubechies, Ten lectures on wavelets, *SIAM*, 1992.
14. I. Daubechies, Orthogonal bases of compactly supported wavelet II. Variation on a theme, *SIAM J. Math. Anal.* **24** (1993) 499–519.
15. D. L. Donoho, Interpolating wavelet transforms, Tech. Rep. 408, Department of Statistics, Stanford University (1992).
16. C. A. Downing, On a solution of the Schrodinger equation with a hyperbolic double-well potential, *J. Math. Phys.* **54** (2013) 072101.
17. K. Fan, W. Cai and X. Ji, A generalized discontinuous Galerkin (GDG) method for Schrodinger equations with nonsmooth solutions, *J. Comput. Phys.* **227** (2008) 2387–2410.
18. J. S. Hesthaven and L. Jameson, A wavelet-optimized adaptive multi-domain method, *J. Comput. Phys.* **145** (1998) 280–296.
19. L. Jameson, A wavelet-optimized, very high order adaptive grid and numerical method, *SIAM J. Sci. Comput.* **19** (1998) 1980–2013.
20. J.-H. Lee and Q. H. Liu, An efficient 3d spectral-element method for Schrodinger equation in nanodevice simulation, *IEEE Trans. Comput. Aided Des. Integr. Circuits Syst.* **24** (2005) 1848–1858.
21. M. Levy, Parabolic equation methods for electromagnetic wave propagation, The Institution of Engineering and Technology, London, UK (2000).
22. Q. H. Liu, C. Cheng and H. Z. Massoud, The spectral grid method: A novel fast Schrodinger-equation solver for semiconductor nanodevice simulation, *IEEE Trans. Comput. Aided Des. Integr. Circuits Syst.* **23** (2004) 1–9.
23. S. Mallat, Multiresolution approximations and wavelet orthonormal bases of L^R, *Trans. Amer. Math. Soc.* **315** (1989) 69–87.
24. M. Mehra and N. K. R. Kevlahan, An adaptive wavelet collocation method for the solution of partial differential equation on the sphere, *J. Comput. Phys.* **227** (2008) 5610–5632.
25. M. Meyer, M. Desbrun, P. Schroder and A. Barr, Discrete differential geometry operator for triangulated 2-manifolds, in: *Visualization and Mathematics III*, Springer, 2003, pp. 35–57.
26. Y. Meyer, *Analysis at Urbana I*: *Analysis in Function Spaces*, Cambridge University Press, Cambridge, 1989.
27. R. Ramesh, M. Madheswaran and K. Kannan, Self-consistent 3d numerical modeling of a uniformly doped nanoscale FinFET using interpolating wavelets, *J. Comput. Electron.* **10** (2011) 331–340.
28. P. Schroder and W. Sweldens, Spherical wavelets: Efficiently representing functions on the sphere, in: *Proceedings of the 22nd Annual Conference on Computer Graphics and Interactive Techniques*, 1995, pp. 161–172.
29. T. Sqrevik, T. Birkeland and G. Oksa, Numerical solution of the 3d time dependent Schrodinger equation in spherical coordinates: Spectral basis and effects of split-operator technique, *J. Comput. Appl. Math.* **225** (2009) 56–67.

30. C. Sulem and P.-L. Sulem, *The Nonlinear Schrodinger Equation*: *Self-focusing and Wave Collapse*, Springer, 1999.
31. E. P. Sumesh and E. Elias, Optimization of finite difference method with multiwavelet bases, *Communications in Computer and Information Science* **40** (2009) 37–48.
32. Y. Suzuki, A. Abedi, N. T. Maitra, K. Yamashita and E. K. U. Gross, Electronic Schrodinger equation with nonclassical nuclei, *Phys. Rev. A* **89** (2014) 040501(R).
33. W. Sweldens, The lifting scheme: A construction of second generation wavelets, *SIAM J. Math. Anal.* **2**(29) (1998) 511–546.
34. O. V. Vasilyev, Solving multi-dimensional evolution problems with localized structure using second generation wavelets, *Int. J. Comp. Fluid Dyn.* **17** (2003) 151–168.
35. O. V. Vasilyev and C. Bowman, Second generation wavelet collocation method for the solution of partial differential equations, *J. Comput. Phys.* **165** (2000) 660–693.
36. E. L. Wachpress, Optimum alterning-direction-implicit iteration parameters for a model problem, *J. Soc. Indust. Appl. Math.* **10** (1962) 339–350.
37. J. Weiss, Applications of compactly supported wavelets to the numerical solution of partial differential equations, in: *Proceedings of the SPIE — The International Society for Optical Engineering*, Vol. 5266.
38. G. Xu, Discrete Laplace-Beltrami operator on sphere and optimal spherical triangulation, *Int. J. Comp. Geometry Appl.* **16** (2006) 75–93.
39. H. Zhu, Y. Chen, S. Song and H. Hu, Symplectic and multi-symplectic wavelet collocation methods for two-dimensional Schrodinger equations, *Appl. Numer. Math.* **61** (2011) 308–321.